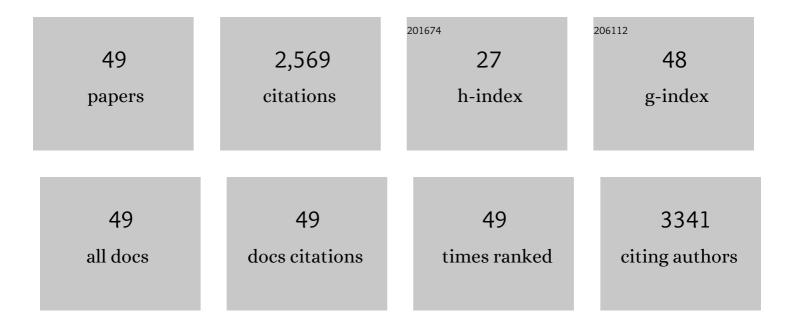
Hionsuck Baik

List of Publications by Year in descending order

Source: https://exaly.com/author-pdf/5145913/publications.pdf Version: 2024-02-01



#	Article	IF	CITATIONS
1	Mnâ€Dopant Differentiating the Ru and Ir Oxidation States in Catalytic Oxides Toward Durable Oxygen Evolution Reaction in Acidic Electrolyte. Small Methods, 2022, 6, e2101236.	8.6	31
2	A Hybrid Zeolite Membrane-Based Breakthrough for Simultaneous CO ₂ Capture and CH ₄ Upgrading from Biogas. ACS Applied Materials & Interfaces, 2022, 14, 2893-2907.	8.0	11
3	Microfluidicsâ€Assisted Synthesis of Hierarchical Cu ₂ O Nanocrystal as C ₂ ‣elective CO ₂ Reduction Electrocatalyst. Small Methods, 2022, 6, e2200074.	8.6	19
4	Understanding the Grain Boundary Behavior of Bimetallic Platinum–Cobalt Alloy Nanowires toward Oxygen Electro-Reduction. ACS Catalysis, 2022, 12, 3516-3523.	11.2	23
5	An Extrinsicâ€Poreâ€Containing Molecular Sieve Film: A Robust, Highâ€Throughput Membrane Filter. Angewandte Chemie - International Edition, 2021, 60, 1323-1331.	13.8	11
6	Mitrofanovite, Layered Platinum Telluride, for Active Hydrogen Evolution. ACS Applied Materials & Interfaces, 2021, 13, 2437-2446.	8.0	10
7	Nanoporous Silver Telluride for Active Hydrogen Evolution. ACS Nano, 2021, 15, 6540-6550.	14.6	10
8	Revealing the Quasi-Periodic Crystallographic Structure of Self-Assembled SnTiS ₃ Misfit Compound. Journal of Physical Chemistry C, 2021, 125, 9956-9964.	3.1	4
9	Vertical-crystalline Fe-doped \hat{l}^2 -Ni oxyhydroxides for highly active and stable oxygen evolution reaction. Matter, 2021, 4, 3585-3604.	10.0	34
10	Crystal Phase Transition Creates a Highly Active and Stable RuC <i>_X</i> Nanosurface for Hydrogen Evolution Reaction in Alkaline Media. Advanced Materials, 2021, 33, e2105248.	21.0	27
11	Pt ²⁺ -Exchanged ZIF-8 nanocube as a solid-state precursor for L1 ₀ -PtZn intermetallic nanoparticles embedded in a hollow carbon nanocage. Nanoscale, 2020, 12, 1118-1127.	5.6	10
12	Intermetallic PtCu Nanoframes as Efficient Oxygen Reduction Electrocatalysts. Nano Letters, 2020, 20, 7413-7421.	9.1	109
13	Stacked CdTe/CdS Nanodiscs via Intraparticle Migration of CdTe on CdS. Chemistry of Materials, 2020, 32, 10104-10112.	6.7	5
14	Highly Crystalline Hollow Toroidal Copper Phosphosulfide <i>via</i> Anion Exchange: A Versatile Cation Exchange Nanoplatform. ACS Nano, 2020, 14, 11205-11214.	14.6	24
15	An unprecedented c-oriented DDR@MWW zeolite hybrid membrane: new insights into H2-permselectivities via six membered-ring pores. Journal of Materials Chemistry A, 2020, 8, 14071-14081.	10.3	10
16	Gold Nanotetrapods with Unique Topological Structure and Ultranarrow Plasmonic Band as Multifunctional Therapeutic Agents. Journal of Physical Chemistry Letters, 2019, 10, 4505-4510.	4.6	30
17	Theoretical and Experimental Understanding of Hydrogen Evolution Reaction Kinetics in Alkaline Electrolytes with Pt-Based Core–Shell Nanocrystals. Journal of the American Chemical Society, 2019, 141, 18256-18263.	13.7	91
18	An Heteroâ€Epitaxially Grown Zeolite Membrane. Angewandte Chemie - International Edition, 2019, 58, 18654-18662.	13.8	38

HIONSUCK BAIK

#	Article	IF	CITATIONS
19	Janus to Core–Shell to Janus: Facile Cation Movement in Cu _{2–<i>x</i>} S/Ag ₂ S Hexagonal Nanoplates Induced by Surface Strain Control. ACS Nano, 2019, 13, 11834-11842.	14.6	23
20	Longitudinal Strain Engineering of Cu2–xS by the Juxtaposed Cu5FeS4 Phase in the Cu5FeS4/Cu2–xS/Cu5FeS4 Nanosandwich. Chemistry of Materials, 2019, 31, 9070-9077.	6.7	12
21	Blue Emission of α-GaN Colloidal Quantum Dots via Zn Doping. Chemistry of Materials, 2019, 31, 5370-5375.	6.7	9
22	Hemi-core@frame AuCu@IrNi nanocrystals as active and durable bifunctional catalysts for the water splitting reaction in acidic media. Nanoscale Horizons, 2019, 4, 727-734.	8.0	43
23	Topotactic Transformations in an Icosahedral Nanocrystal to Form Efficient Waterâ€ 6 plitting Catalysts. Advanced Materials, 2019, 31, e1805546.	21.0	76
24	NiOOH Exfoliation-Free Nickel Octahedra as Highly Active and Durable Electrocatalysts Toward the Oxygen Evolution Reaction in an Alkaline Electrolyte. ACS Applied Materials & Interfaces, 2018, 10, 10115-10122.	8.0	68
25	Dendrite-Embedded Platinum–Nickel Multiframes as Highly Active and Durable Electrocatalyst toward the Oxygen Reduction Reaction. Nano Letters, 2018, 18, 2930-2936.	9.1	121
26	Vertexâ€Reinforced PtCuCo Ternary Nanoframes as Efficient and Stable Electrocatalysts for the Oxygen Reduction Reaction and the Methanol Oxidation Reaction. Advanced Functional Materials, 2018, 28, 1706440.	14.9	161
27	RuO _x -decorated multimetallic hetero-nanocages as highly efficient electrocatalysts toward the methanol oxidation reaction. Nanoscale, 2018, 10, 21178-21185.	5.6	21
28	Highly Crystalline Pd ₁₃ Cu ₃ S ₇ Nanoplates Prepared via Partial Cation Exchange of Cu _{1.81} S Templates as an Efficient Electrocatalyst for the Hydrogen Evolution Reaction. Chemistry of Materials, 2018, 30, 6884-6892.	6.7	36
29	Partial Edge Dislocations Comprised of Metallic Ga Bonds in Heteroepitaxial GaN. Nano Letters, 2018, 18, 4866-4870.	9.1	5
30	An IrRu alloy nanocactus on Cu _{2â^'x} S@IrS _y as a highly efficient bifunctional electrocatalyst toward overall water splitting in acidic electrolytes. Journal of Materials Chemistry A, 2018, 6, 16130-16138.	10.3	58
31	A facet-controlled Rh ₃ Pb ₂ S ₂ nanocage as an efficient and robust electrocatalyst toward the hydrogen evolution reaction. Nanoscale, 2018, 10, 9845-9850.	5.6	28
32	Janus Nanoparticle Structural Motif Control <i>via</i> Asymmetric Cation Exchange in Edge-Protected Cu _{1.81} S@Ir _{<i>x</i>} S _{<i>y</i>} Hexagonal Nanoplates. ACS Nano, 2018, 12, 7996-8005.	14.6	36
33	Cobalt Assisted Synthesis of IrCu Hollow Octahedral Nanocages as Highly Active Electrocatalysts toward Oxygen Evolution Reaction. Advanced Functional Materials, 2017, 27, 1604688.	14.9	186
34	Cactusâ€Like Hollow Cu _{2â€} <i>_x</i> S@Ru Nanoplates as Excellent and Robust Electrocatalysts for the Alkaline Hydrogen Evolution Reaction. Small, 2017, 13, 1700052.	10.0	86
35	Iridium-Based Multimetallic Nanoframe@Nanoframe Structure: An Efficient and Robust Electrocatalyst toward Oxygen Evolution Reaction. ACS Nano, 2017, 11, 5500-5509.	14.6	243
36	Radially Phase Segregated PtCu@PtCuNi Dendrite@Frame Nanocatalyst for the Oxygen Reduction Reaction. ACS Nano, 2017, 11, 10844-10851.	14.6	110

HIONSUCK BAIK

#	ARTICLE	IF	CITATIONS
37	Lanthanide metal-assisted synthesis of rhombic dodecahedral MNi (M = Ir and Pt) nanoframes toward efficient oxygen evolution catalysis. Nano Energy, 2017, 42, 17-25.	16.0	94
38	Synthesis of compositionally tunable, hollow mixed metal sulphide Co _x Ni _y S _z octahedral nanocages and their composition-dependent electrocatalytic activities for oxygen evolution reaction. Nanoscale, 2017, 9, 15397-15406.	5.6	52
39	Plasmon Enhanced Direct Bandgap Emissions in Cu ₇ S ₄ @Au ₂ S@Au Nanorings. Small, 2016, 12, 5728-5733.	10.0	16
40	Rational design of Pt–Ni–Co ternary alloy nanoframe crystals as highly efficient catalysts toward the alkaline hydrogen evolution reaction. Nanoscale, 2016, 8, 16379-16386.	5.6	128
41	Facet-controlled hollow Rh ₂ S ₃ hexagonal nanoprisms as highly active and structurally robust catalysts toward hydrogen evolution reaction. Energy and Environmental Science, 2016, 9, 850-856.	30.8	118
42	Rational Synthesis of Heterostructured M/Pt (M = Ru or Rh) Octahedral Nanoboxes and Octapods and Their Structure-Dependent Electrochemical Activity Toward the Oxygen Evolution Reaction. Small, 2015, 11, 4462-4468.	10.0	32
43	Scalable synthesis of djurleite copper sulphide (Cu _{1.94} S) hexagonal nanoplates from a single precursor copper thiocyanate and their photothermal properties. CrystEngComm, 2015, 17, 4627-4631.	2.6	36
44	Skeletal Octahedral Nanoframe with Cartesian Coordinates <i>via</i> Geometrically Precise Nanoscale Phase Segregation in a Pt@Ni Core–Shell Nanocrystal. ACS Nano, 2015, 9, 2856-2867.	14.6	176
45	Facet-controlled {100}Rh–Pt and {100}Pt–Pt dendritic nanostructures by transferring the {100} facet nature of the core nanocube to the branch nanocubes. Nanoscale, 2015, 7, 3941-3946.	5.6	18
46	Synthesis and sonication-induced assembly of Si-DDR particles for close-packed oriented layers. Chemical Communications, 2013, 49, 7418.	4.1	20
47	Fabrication of hierarchical Rh nanostructures by understanding the growth kinetics of facet-controlled Rh nanocrystals. Chemical Communications, 2013, 49, 2225.	4.1	29
48	Uniform Siâ€CHA Zeolite Layers Formed by a Selective Sonicationâ€Assisted Deposition Method. Angewandte Chemie - International Edition, 2013, 52, 5280-5284.	13.8	31
49	Vertical Alignment of Fe-Doped <i>β</i> â€'Ni Oxyhydroxides for Highly Active and Stable Oxygen Evolution Reaction. SSRN Electronic Journal, 0, , .	0.4	0